Identification and validation of critical mitochondrial hub genes for prostate cancer

SHA LIU[1], LIANG HUANG[1], LI LIN[1], HONG SHAN[2] and YUEMING WAN[3]

[1]Department of Urology, The Affiliated Cancer Hospital of Xiangya School of Medicine (Hunan Cancer Hospital), Central South University, Changsha, Hunan 410013, P.R. China; [2]Department of Emergency Medicine, The Affiliated Changsha Central Hospital, Hengyang Medical School, University of South China, Changsha, Hunan 410028, P.R. China; [3]Department of Urology, Yueyang Hospital Affiliated to Hunan Normal University (Yueyang People's Hospital), Yueyang, Hunan 414000, P.R. China

Received May 30, 2025; Accepted November 3, 2025

DOI: 10.3892/ol.2025.15419

Abstract. Prostate cancer (PCa) is one of the most common malignant tumors in men. In recent years, mitochondrial dysfunction has been found to be closely related to cancer progression. However, the role of mitochondria-related genes in PCa remains unclear. The aim of the present study was to discover novel biomarkers based on differentially expressed mitochondrial-related genes (DeMRGs) to aid in PCa diagnosis. In the present study, gene expression data from the Gene Expression Omnibus and The Cancer Genome Atlas databases were combined with a mitochondrial-related gene list provided by the MitoCarta database to identify DeMRGs. Gene Ontology analysis, Kyoto Encyclopedia of Genes and Genomes enrichment analysis and Gene Set Enrichment Analysis were then used to investigate the functions and related pathways of these DeMRGs. Subsequently, Cytoscape software and the STRING website were used to explore the transcription factors and microRNAs related to the DeMRGs. The degree of infiltration of immune cells in the immune landscape of patients with PCa and the controls was assessed using CIBERSORT. Finally, the correlation between characteristic DeMRGs and immune cell infiltration and mitochondrial respiration was analyzed. The results indicated that 6 characteristic genes, including acetyl-CoA carboxylase β (ACACB), pyruvate dehydrogenase kinase 4 (PDK4), glycine amidinotransferase (GATM), methylcrotonyl-CoA carboxylase subunit 2, mitochondrial ribosomal protein L12 (MRPL12) and fatty acid synthase, were identified from the 60 DeMRGs. The results showed a close association between the characteristic DeMRGs and immune infiltrating cells. In addition, it was found that MRPL12, PDK4, ACACB and GATM were correlated with mitochondrial respiration. These 4 genes were selected as hub genes as they are closely related to gluconeogenesis, the tricarboxylic acid cycle, lipid metabolism, amino acid metabolism and other mitochondrial metabolic pathways in PCa. In conclusion, 4 novel mitochondrial-related gene signatures that influence mitochondrial metabolism within the immune microenvironment were identified in PCa.

Correspondence to: Dr Hong Shan, Department of Emergency Medicine, The Affiliated Changsha Central Hospital, Hengyang Medical School, University of South China, 161 South Shaoshan Road, Changsha, Hunan 410028, P.R. China
E-mail: shirleyv5@163.com

Key words: prostate cancer, mitochondrial related genes, mitochondrial respiration, mitochondria metabolism

Introduction

According to the latest tumor epidemiological statistics, prostate cancer (PCa) is still the most common tumor affecting male reproductive and urinary health, with its incidence rate and mortality ranking fourth and eighth, respectively (1). PCa progresses slowly in the early stages and surgical resection, radiation therapy and androgen deprivation therapy can effectively halt the progression of disease. However, approximately one-third of patients with PCa develop recurrence or metastasis after radical surgery. These patients can be treated with androgen-deprivation therapy, also known as castration therapy, which involves the administration of gonadotropin-releasing hormone agonists, or with surgical castration (2). Unfortunately, most patients develop disease progression again ~18 months after treatment and are no longer affected by androgen levels. Instead, the disease evolves into a more aggressive form of castration-resistant PCa, either metastatic castration-resistant disease or non-metastatic castration-resistant disease (3). The first-line treatment for castration-resistant PCa mainly includes the chemotherapy drug docetaxel along with novel endocrine drugs, such as abiraterone or enzalutamide (4). Although the early treatment response is good, drug resistance is still inevitable in the later stages and no effective treatment exists for these patients at present. Therefore, it is important to explore the molecular mechanisms of PCa progression (5).

Mitochondria are responsible for the synthesis of intracellular bioenergetics. In addition to the synthesis of ATP, mitochondria can also synthesize macromolecular metabolic precursors, such as lipids, proteins, DNA and RNA. Mitochondria can also remove or use metabolic waste, such as reactive oxygen species (ROS) and gases (6). Under normal

physiological conditions, mitochondria are important cell pressure sensors and can coordinate cell adaptation to various stressors, such as nutrient deprivation, oxidative stress, DNA damage and endoplasmic reticulum stress. Therefore, mitochondria can maintain the growth and survival of tumor cells in harsh environments, including nutrient depletion, hypoxia and tumor treatment, which is a key factor in promoting tumor progression (7). An early study found that tumor cells still tended to undergo glycolysis under aerobic conditions, known as the Warburg effect, indicating that mitochondrial respiratory defects may be the fundamental cause of tumor development. In recent years, mitochondrial function and tumor metabolism reprogramming have received increasing attention (8). Researchers have found that the Warburg effect is not a characteristic of all cancer cells. Although damaged mitochondria may drive the Warburg effect in some cases, a number of tumor cells that exhibit Warburg metabolism also have complete mitochondrial respiration and some tumor subtypes also depend on mitochondrial respiration (7,9). Biosynthesis and other functions of mitochondria are typically upregulated in cancer and metabolic reprogramming has become an important tumor marker (10). The metabolic phenotype of prostate epithelial cells is unique and the stages of tumor development and progression from prostatic intraepithelial neoplasia to metastasis are different. Normal prostate epithelial cells are highly dependent on glycolysis, but during tumor progression, PCa cells gradually reactivate mitochondrial oxidative phosphorylation while increasing glucose metabolism and reducing citrate production (11,12). In PCa, androgen receptors (ARs) also participate in cellular metabolic reprogramming, which includes aerobic glycolysis, mitochondrial respiration and *de novo* fat generation, thereby meeting the metabolic and biosynthetic needs of PCa cells (13,14).

In the present study, differentially expressed genes (DEGs) in PCa were first identified by analyzing three datasets: The Cancer Genome Atlas (TCGA)-prostate adenocarcinoma (PRAD), GSE46602 and GSE55945. This initial step focused on screening general DEGs (upregulated or downregulated) between PCa and adjacent normal tissues across the datasets, without restricting to mitochondrial relevance. To narrow down the identified DEGs to mitochondria-associated candidates, the first intersection was performed by overlapping these general PCa DEGs with the full list of human mitochondrial protein-coding genes from the MitoCarta3.0 database. This step yielded a preliminary set of differentially expressed mitochondrial-related genes (DeMRGs) but still included all genes that met both 'differential expression in PCa' and 'mitochondrial localization' criteria. To further refine and prioritize high-confidence targets, a second targeted intersection was conducted: The upregulated subset of the initially obtained DeMRGs was re-intersected with the MitoCarta3.0 mitochondrial gene list. This distinct step aimed to exclude potential false positives and focus specifically on consistently upregulated DeMRGs, a subset with stronger relevance to PCa progression as upregulated mitochondrial genes are more likely to drive pro-tumor metabolic reprogramming. Subsequently, Gene Ontology (GO) and Kyoto Encyclopedia of Genes and Genomes (KEGG) analyses were performed on these DeMRGs. The transcription factors and microRNAs (miRNAs) associated with the DEGs were also analyzed to provide a basis for further mechanistic studies. Furthermore, to explore the role of mitochondrial-related genes in PCa, the present study analyzed the correlation between key mitochondrial genes and immune infiltration through immune infiltration analysis. Additionally, it investigated the association of these genes with mitochondrial respiration and their relationship with mitochondrial metabolic pathways in PCa, aiming to identify potential mitochondrial hub genes involved in PCa progression.

Materials and methods

Cell culture. The PCa cell lines (Du145, PC-3 and LNcap) and normal prostate cells (RWPE-1) purchased from American Type Culture Collection) were cultured in medium containing 10% fetal bovine serum (Gibco; Thermo Fisher Scientific, Inc.) at 37˚C constant temperature and 5% CO_2. Du145 cells were maintained in MEM (Biotecnómica), whereas PC-3 and LNcap were maintained in RPMI (Biotecnómica) and RWPE-1 was maintained in K-SFM (Biotecnómica).

Reverse transcription-quantitative PCR (RT-qPCR). Total RNA was extracted from the RWPE-1, PC-3, LNcap and Du145 cell lines using RNAiso Plus reagent (Thermo Fisher Scientific, Inc.). cDNA was synthesized using a PrimeScript™ RT reagent kit (Takara Biotechnology Co., Ltd) at 42˚C for 15 min and 85˚C for 5 sec. Two-step qPCR was performed using SYBR Green Reagent (Takara Biotechnology Co., Ltd.), C1000 Touch Thermal Cycler and the CFX96 Real-Time System according to the manufacturer's instructions. The primer sequences are listed in Table I. The results were calculated using the $2^{-\Delta\Delta Cq}$ method, and the data are expressed as a ratio of the control gene GAPDH (15).

Public data acquisition and preprocessing. RNA-sequencing (RNA-seq) data for patients with PCa were derived from the TCGA-PRAD dataset (TCGA-PRAD; https://www.cancer.gov/about-nci/organization/ccg/research/structural-genomics/tcga), which includes 502 cancer tissues and 52 adjacent tissues, and from two datasets provided by the National Center for Biotechnology Information Gene Expression Omnibus (https://www.ncbi.nlm.nih.gov/geo): GSE46602 (consisting of 36 cancer tissues and 14 adjacent tissues) and GSE55945 (including sequencing data from 13 cancer tissues and 8 adjacent tissues) (16,17). In addition, the GSE70770 dataset was used as an independent validation cohort, which contains RNA-seq data for 220 PCa tissues and 73 adjacent non-cancerous tissues (18). Using R v4.2.2 (https://cran.r-project.org/), the array datasets were normalized using the limma package v3.58.1 and high-throughput sequencing count data were normalized using DESeq2 (version 3.20.0) to generate standardized matrices. Specifically, the DESeq function was applied for normalization, which accounts for library size differences and adjusts for gene-wise dispersion estimates. For genes with multiple transcript IDs, the ID with the highest average expression was selected. The original gene expression data underwent log2 transformation and quantile normalization for subsequent downstream analyses.

Identification and functional enrichment analysis of DeMRGs. The DEGs found in PCa and adjacent tissues were analyzed

Table I. Sequences of the reverse transcription-quantitative PCR primers.

Genes	Forward (5'-3')	Reverse (5'-3')
ACACB	AGATCGCCTCCACCGTTGTC	CTGTCACCTCACCTGTCTTCTACT
PDK4	TGAGTGTTCAAGGATGCTCTGTG	GGTCTGGTTGGTTAAGTGTAGCA
GATM	TCATTGGACCTGGTATTGTGCTTTC	GTAATGAGGAGGTTGTGGTTAGT AGG
MCCC2	AGGTGGCATTATTACAGGCATTGG	CGGATGATGGGTCACTGACACTT
MRPL12	ACATCGCCAGCCTCACTCTC	GGCTACCCACCACACTACAGA
FASN	CAGCGGCAAGCGTGTGATG	GTTGACCTGCGACCTCCTCC
GAPDH	AATGGGCAGCCGTTAGGAA	GAGACTAAACCAGCATAACCCG

ACACB, acetyl-CoA carboxylase β; PDK4, pyruvate dehydrogenase kinase 4; GATM, glycine amidinotransferase; MCCC2, methylcrotonyl-CoA carboxylase subunit 2; MRPL12, mitochondrial ribosomal protein L12; FASN, fatty acid synthase.

using the limma and DESeq2 packages, with the following selection criteria: $\log_2$|fold change|≥1 and P<0.05. DeMRGs were identified by intersecting these DEGs (from TCGA-PRAD, GSE46602 and GSE55945) with 1,136 human mitochondrial protein-coding genes from MitoCarta3.0 (https://www.broadinstitute.org/mitocarta/mitocarta30-inventory-mammalian-mitochondrial-proteins-and-pathways), visualized via heat maps, Venn diagrams and volcano plots. GO (http://geneontology.org) and KEGG (https://www.genome.jp/kegg/kegg1.html) enrichment analyses of DeMRGs were performed using R's clusterProfiler package (v4.10.1). Gene Set Enrichment Analysis (GSEA; https://www.broadinstitute.org/gsea/) with KEGG gene sets (c2.cp.KEGG.v7.4.symbols.gmt from MSigDB; http://software.broadinstitute.org/gsea/msigdb/) was conducted, with significance defined as P<0.05 and false discovery rate <0.05. The transcription factors and interacting miRNAs of the identified DeMRGs were predicted using the online platform NetworkAnalyst 3.0 (https://www.networkanalyst.ca/) and visualized with Cytoscape software.

Protein-protein interaction (PPI) analysis and hub gene extraction. In the present study, PPI networks of DeMRGs were identified to determine the differences between PCa and its adjacent tissues from the perspective of protein interactions. First, the STRING online analysis tool (https://www.string-db.org/) was used to generate the PPI network of DeMRGs. Then, the PPI network was analyzed using Cytoscape software (https://cytoscape.org; CytoHubba plugin and DMNC; v3.10.0) and screened out genes with a degree value ≥4 as core genes for further research. The network type was full STRING. In total, six core data sources were integrated to ensure interaction reliability, including 'experiments', 'databases', 'co-expression', 'neighborhood', 'gene fusion' and 'co-occurrence'. The interaction score was set to a confidence threshold of 0.4.

Hub genes and PCa immune infiltration analysis. The TCGA-PRAD differential gene volcano plot was generated using R's ggplot2 (https://CRAN.R-project.org/package=ggplot2; v3.5.1). Core DeMRGs in TCGA-PRAD were obtained by intersecting TCGA-PRAD DEGs with core genes. For immune infiltration analysis, R was used to convert count data to transcripts per million (TPM), followed by the use of CIBERSORT (http://cibersort.stanford.edu; v3.15.0) to estimate 22 immune cell proportions (P<0.05 was considered reliable). The correlation between each hub gene and the 22 immune cell types was tested using Spearman's rank correlation analysis and visualized as lollipop plots. GSEA with KEGG analysis were used for functional enrichment. Using the GSE70770 dataset, the immune infiltration scores for 22 immune cell subsets were calculated via single-sample GSEA (ssGSEA) implemented through the R package Gene Set Variation Analysis (GSVA). Specifically, the GSVA package was used to run ssGSEA, which quantifies the enrichment level of each immune cell-associated gene set within individual samples of GSE70770, thereby generating the immune infiltration scores for each cell type. Paired t-tests were used to compare the immune scores of PCa and adjacent tissues, visualized as box plots with R's ggplot2. Immune cell composition was also plotted with R's ggplot2. Spearman correlation tests of genes and immune cells were visualized as heat maps using R's ComplexHeatmap (v1.0.12). To ensure the reliability of the observed correlations across different computational tools, R's psych package (v2.4.3) was used to compute correlation coefficients and P-values of core DeMRGs and immune cells; box plots showed the differences in the immune scores of high/low expression (samples with expression levels greater than or equal to the median were defined as the high expression subgroup, while those with expression levels below the median were designated as the low expression subgroup.) subgroups. Cluster analysis heat maps (using the pheatmap v1.0.12 function in R) illustrated the relationships between hub gene expression and immune cells. The correlations between the 6 core genes and immune cells were calculated using the R package Hmisc (v5.1-1).

Bioinformatics evaluation of the PCa mitochondrial respiratory chain and mitochondrial metabolism. Using MitoCarta3.0 and TCGA-PRAD data, paired t-tests were conducted to identify genes with significant differences (P<0.05) in oxidative respiratory chain complexes in cancer cells and adjacent tissues, visualized via R's ggplot2. Genes that were |statistical|>6 were correlated with the CIBERSORT immune infiltration results, with correlation heat maps generated using ggplot2. Spearman rank analysis was conducted to

assess the correlations between the 6 hub genes and oxidative respiratory chain complex genes (|statistical|>4); these correlations were visualized using ggplot2. Linear regression was used to evaluate the pairwise relationships between the 4 selected hub genes and oxidative phosphorylation (OXPHOS) genes. R's ggplot2 (stat_compare_means) was used to perform paired t-tests to analyze the expression of damage associated molecular patterns DAMPs genes (such as BCL2 and calreticulin) and immune receptor-related genes (such as toll-like receptor 2 and cyclic GMP-AMP synthase). Mantel tests and Pearson correlations were used to calculate the correlations between the 4 hub genes, mitochondrial metabolism and DAMPs.

Statistical analyses. SPSS 20.0 (IBM Corp.) was utilized to perform the statistical analyses. Data are shown as the mean ± standard error of the mean according to the results of three independent repeated experiments. One-way analysis of variance (ANOVA) was employed to analyze differences in the expression levels of the 6 core DeMRGs [acetyl-CoA carboxylase β (ACACB), pyruvate dehydrogenase kinase 4 (PDK4), glycine amidinotransferase (GATM), methylcrotonyl-CoA carboxylase subunit 2 (MCCC2), mitochondrial ribosomal protein L12 (MRPL12) and fatty acid synthase (FASN)] in the four different cell lines, which were detected by RT-qPCR from three independent repeated experiments. Following the one-way ANOVA, the Tukey's honestly significant difference test was used as the post hoc test to perform pairwise comparisons between groups, ensuring the accurate identification of specific differences in gene expression levels among different cell lines and between different genes. $P<0.05$ was considered to indicate a statistically significant difference.

Results

Identification of DeMRGs in PCa and enrichment analyses. TCGA-PRAD contains RNA-seq data for 554 tissue samples, including 502 cancer tissues and 52 adjacent tissues. Differential analysis identified 1,681 genes that were significantly downregulated and 1,216 genes that were significantly upregulated in PCa. The DEGs were intersected with human mitochondrial genes in the MitoCarta3.0 database to obtain 60 intersecting genes, including 34 significantly upregulated and 26 significantly downregulated genes. The top 9 DeMRGs are shown in Fig. 1A. Similarly, 523 genes were significantly downregulated and 323 genes were significantly upregulated in PCa in GSE46606 and 337 genes were significantly downregulated and 191 genes were significantly upregulated in PCa in GSE55945. After taking the intersection of these DEGs with the MitoCarta3.0 database, 23 significantly upregulated and 22 significantly downregulated genes were identified in GSE46602, while 4 significantly upregulated and 23 significantly downregulated genes were identified in GSE55945 (Fig. 1A). After conducting a differential analysis using the training set (TCGA-PRAD, GSE 46606 and GSE55945), To specifically screen for high-confidence upregulated mitochondria-related genes in PCa, the upregulated subset of the initially identified 60 DeMRGs (from intersecting general PCa DEGs with MitoCarta3.0 mitochondrial genes) was further intersected with the human mitochondrial genes in the MitoCarta3.0 database. This targeted refinement yielded 6 core upregulated mitochondrial genes, which were selected for subsequent functional and correlation analyses. The 6 mitochondrial genes in GSE55945 and GSE46602 are presented as heat maps (Fig. 1B).

GO analysis was performed on all significantly upregulated DeMRGs (54 genes) in the three datasets, including in terms of molecular function, biological process and cell component. This analysis showed that the DeMRGs significantly upregulated in PCa were related to 'nucleotide phosphate metabolic process', 'oxidative phosphorylation', 'mitochondrial transport', 'mitochondrial transmembrane transport' and 'ribosomes' (Fig. S1A). By contrast, the 63 significantly downregulated DeMRGs in PCa were associated with 'small molecule catabolic process', 'organic acid biosynthetic process' and 'mitochondrial gene expression' (Fig. S1B).

Correlation analysis of core genes. KEGG analysis and GSEA showed that the upregulated DeMRGs were enriched in multiple metabolic pathways and were associated with multiple diseases, including 'Huntington' disease', 'Parkinson disease' and 'prion diseases' (Fig. 2A and B). Similarly, the KEGG and GSEA results showed that the downregulated DeMRGs were enriched in multiple metabolic pathways and 'PPAR signaling pathway' (Fig. 2C and D). A PPI network was constructed using the STRING website to analyze the 54 upregulated genes and Cytoscape analysis was used to screen out 18 core genes with a degree value >4 (Fig. 3A). Subsequently, NetworkAnalyst 3.0 was used to predict the transcription factors and interacting miRNAs of these 18 genes (Fig. 3B). Similarly, the 63 downregulated genes were used to construct a PPI network through the STRING website and 16 genes were screened out based on a degree value >4 (Fig. 3C). The predicted transcription factors and interacting miRNAs of these 16 genes were also screened out (Fig. 3D). The results collectively suggest that the core genes selected in the present study are related to multiple transcription factors and miRNAs.

Correlation between core DeMRGs and immune infiltration in PCa. The TPM expression matrix of PCa tissue (502 cases) was used to calculate its immune score using the CIBERSORT deconvolution algorithm. The genes examined are the intersection of the 60 DeMRGs in TCGA-PRAD and the 34 core upregulated genes selected earlier, resulting in 15 intersection genes, which were the core DeMRGs of TCGA-PRAD. Subsequently, using the TPM expression matrix of PCa tissues (502 cases) from TCGA-PRAD dataset, the proportions of 22 immune cell subsets were first estimated via the CIBERSORT deconvolution algorithm to generate immune infiltration profiles. On this basis, a correlation analysis was further performed between these 15 intersection genes and the aforementioned immune infiltration results (Fig. 4A). It can be observed that there are significant differences in the positive and negative correlations between different immune cells and specific genes. These differences help to reveal the association between immune cell functions and gene expression, and provide references for research on tumor immune regulation, gene functions and other related fields. The 6

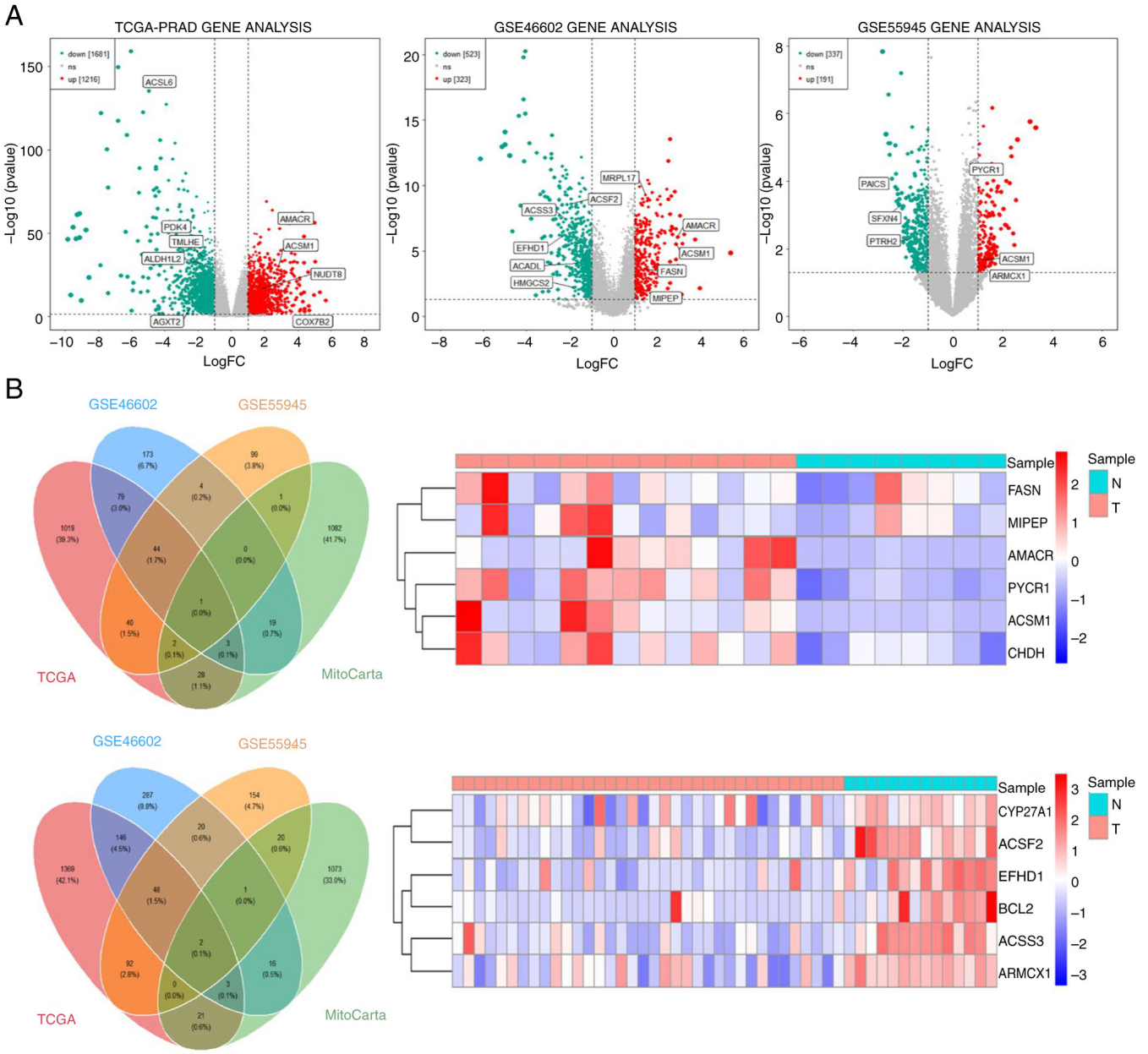

Figure 1. Differential expression of mRNA in mitochondria between prostate cancer and normal prostate tissue. (A) Differential analysis was conducted on three training sets (TCGA-PRAD, GSE46602 and GSE55945). (B) The left sides are the Venn diagram, and the right side is the expression heatmap. The top images are for GSE55945 and the bottom images are for GSE46602; TCGA, The Cancer Genome Atlas; PRAD, prostate adenocarcinoma; ns, no significance; FASN, fatty acid synthase; MIPEP, mitochondrial intermediate peptidase; AMACR, α-methylacyl-CoA racemase; PYCR1, pyrroline-5-carboxylate reductase 1; ACSM1, acyl-CoA synthetase medium chain family member 1; CHDH, choline dehydrogenase; N, normal; T, tumor; FC, fold change.

genes most closely related to immunity were screened out, as shown in Fig. 4B. The differences in the expression of the 6 genes in PCa and adjacent tissues were significant. ACACB, PDK4 and GATM were downregulated in PCa, while MCCC2, MRPL12 and FASN were upregulated in PCa. Lollipop plots of the 6 genes were constructed and the results showed a significant negative correlation between MRPL12 and quiescent CD4 memory T cells, memory B cells and M1 macrophage infiltration, while the trend was the opposite for Tregs and NK-activated cells ($P<0.05$; Fig 4C). MCCC2 was significantly negatively correlated with the infiltration of memory B cells, activated dendritic cells and Tregs cells, while the trend was the opposite for plasma cells and stationary mast cells ($P<0.05$; Fig. 4D). A significant negative correlation was found between FASN and γ-δ T cells, quiescent CD4 memory T cells and memory B cells, while the opposite was found for plasma cells and M0 macrophages ($P<0.05$; Fig. 4E). PDK4 was significantly negatively correlated with Tregs, memory B cells and follicular helper T cells, while it was positively correlated with activated mast cells, resting $CD4^+$ memory T cells and CD8 T cells (Fig. 4F). GATM was significantly negatively correlated with plasma cells and Tregs, while it was positively correlated with resting $CD4^+$ memory T cells, resting dendritic cells and γ-δ T cells (Fig. 4G). ACACB was significantly negatively correlated with Tregs, plasma

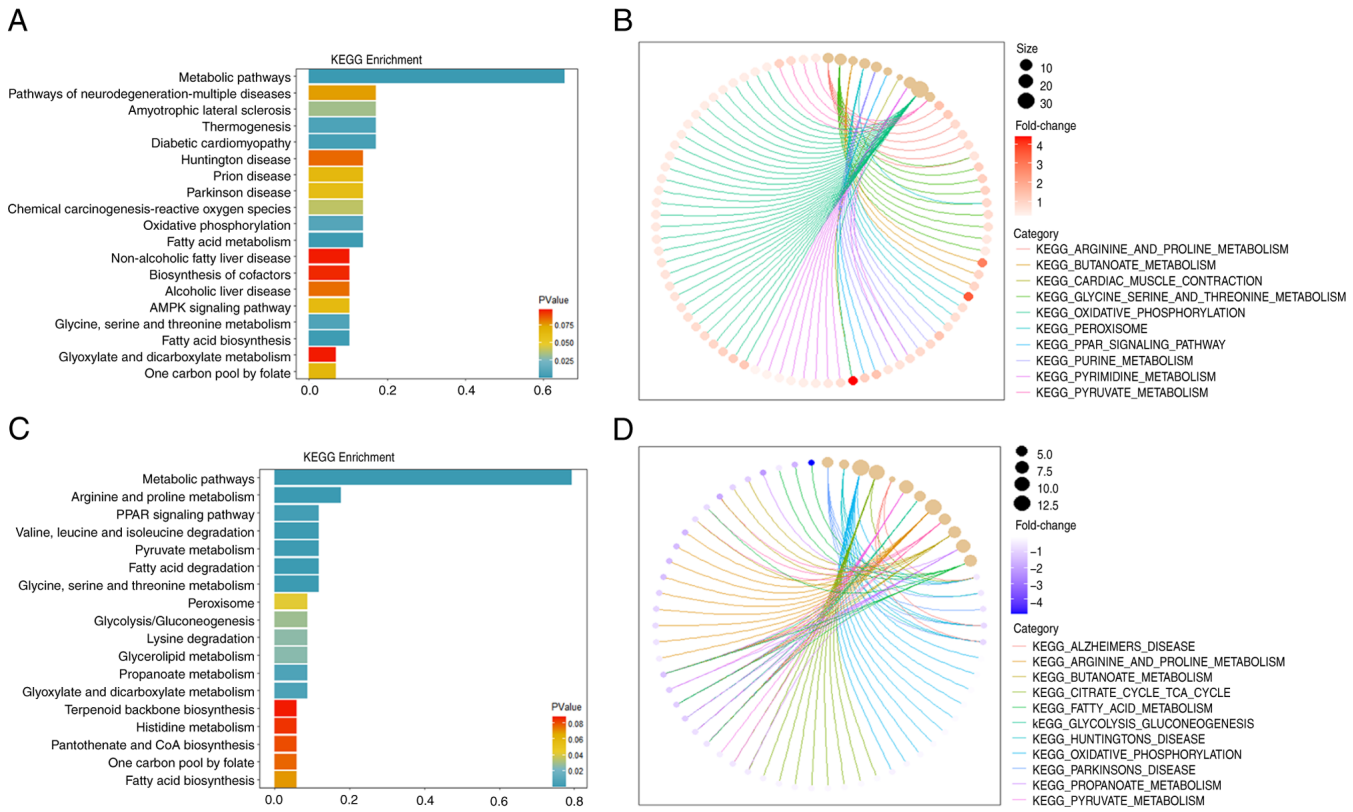

Figure 2. KEGG analysis and GSEA of differential mitochondrial mRNA between prostate cancer and normal prostate tissue. (A) KEGG enrichment analysis of upregulated mitochondrial genes; (B) GSEA of upregulated mitochondrial genes; (C) KEGG enrichment analysis of downregulated mitochondrial genes; and (D) GSEA of downregulated mitochondrial genes. KEGG, Kyoto Encyclopedia of Genes and Genomes; GSEA, Gene Set Enrichment Analysis.

cells and M2 macrophages, while it was positively correlated with resting CD4$^+$ memory T cells, resting dendritic cells and activated dendritic cells (Fig. 4H). Subsequently, a single-gene GSEA was conducted; the results showed that MCCC2, MRPL12 and FASN were negatively correlated with 'KEGG_APOPTOSIS', 'KEGG_B_CELL_RECEPTOR_SIGNALING_PATHWAY' and 'KEGG_INTESINAL_IMMUNE_NETWORK_FOR_IGA_PRODUCTION'. However, ACACB, PDK4 and GATM showed the opposite results (Fig. S2). These results imply a close association between the core DeMRGs and infiltrating immune cells.

Validation of the correlation between the 6 characteristic genes and immune cell infiltration. GSE70770 was used for validation, which included a total of 293 tissue samples: 220 PCa tissues and 73 adjacent cancer samples. The results showed that in PCa, the 6 genes were significantly downregulated in activated B cells, effector CD8 memory T cells, immature dendritic cells, mast cells and NK cells of PCa tissues compared with the adjacent cancer tissues (Fig. 5A). Next, the proportion of 26 immune cells in PCa and adjacent tissues were analyzed using the GSE70770 dataset (Fig. 5B). There were significant stratified differences in the proportions of different types of immune cells (such as activated B cells, activated CD4/CD8 T cells, macrophages and neutrophils) between the two types of tissues. These observed differences are suggestive of immune cell remodeling within the tumor microenvironment, thereby providing critical insights that hold value for investigating the molecular mechanisms underlying tumor immune escape and identifying candidate targets for immune-based therapeutic interventions. The correlation between the 6 core genes and immune cells were calculated using the Hmisc R package and displayed it in the form of a heat map (Fig. 5C). The results showed that these genes were correlated (P<0.001) with NK cells, NK-T cells, B cells, dendritic cells, mast cells and CD8 memory T cells. The correlation coefficients and P-values for these 6 genes and the immune cells were calculated separately. The results showed that high expression of MCCC2, MRPL12 and FASN was associated with low expression of activated B cells, CD8 memory T cells, NK cells and NK-T cells. In addition, low expression of PDK4, ACACB and GATM was associated with low expression of activated B cells, CD8 memory T cells, NK cells and NK-T cells; the strongest immune correlation was with GATM (Fig. 6A). A heat map was used to visually display the differences between cancer and the adjacent immune cells, as well as the relationship between the expression levels of these 6 core genes and immune cells. The results showed that with low expression of PDK4 and GATM, memory B cells and CD4 memory T cells were highly expressed, while CD8 memory T cells showed lower expression levels (Fig. 6B).

Relationship between the 6 core genes, mitochondrial respiration and PCa progression. Next, the TCGA-PRAD dataset was used to study the relationship between mitochondrial respiration and PCa as well as its relationship with the 6 core genes and selected statistically significant genes (P<0.05; Fig. 7A).

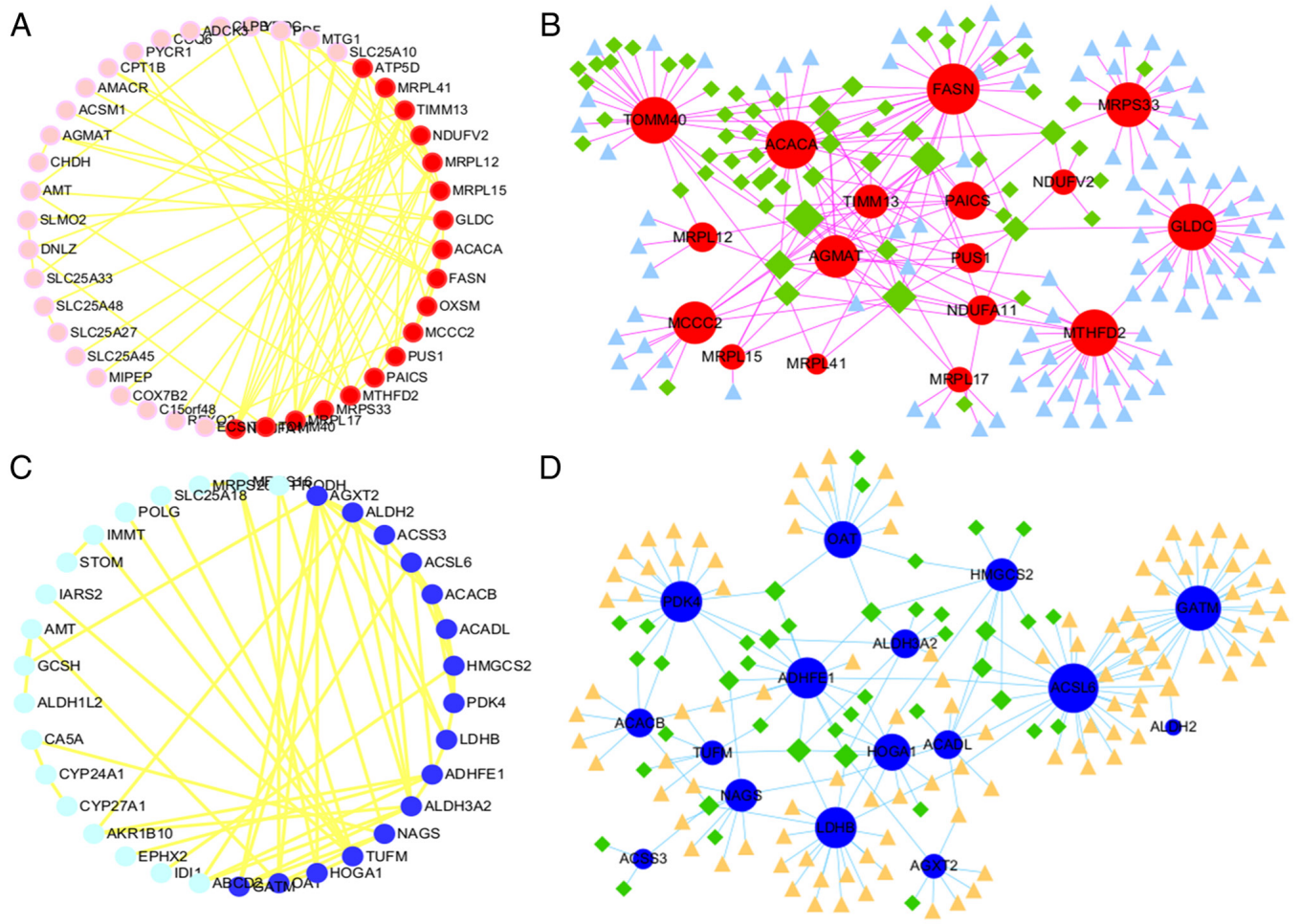

Figure 3. Interaction between differential mRNA and miRNA and transcription factors between prostate cancer and normal prostate tissue. (A) The 54 upregulated genes were first used to construct a PPI network through the STRING website, which was then imported into Cytoscape to screen out 18 core genes with a degree value >4, namely the genes shown in red on the right; (B) The transcription factor and miRNA interactions of these 18 genes predicted by the NetworkAnalyst 3.0 website. Red represents the 18 core genes, and the larger the degree value, the larger the circle size. Green represents the transcription factors and light blue represents miRNA. (C) The 63 downregulated genes were first constructed into a PPI network through the STRING website, which was then imported into Cytoscape to screen out 16 core genes with a degree value >4, namely the genes in dark blue on the right; (D) The transcription factors and interacting miRNAs of these 16 genes were predicted by NetworkAnalyst 3.0 and visualized by Cytoscape. Blue represents the 16 core genes, with larger degree values shown with larger circles. Green represents the transcription factors and the pale orange represents miRNAs. miRNA, microRNA; PPI, protein-protein interaction.

Genes such as COX10, COX11 and COX14 were upregulated, while genes such as FOXRED1, AGOX3 and FMC1 showed a downward trend. Genes with |statistical|>6 were selected and their correlation with immune infiltrating cells was calculated using CIBERSORT. The results showed that these mitochondrial respiratory chain genes were negatively correlated with resting CD4 memory T cells and positively correlated with Tregs (Fig. 7B). Using the TCGA-PRAD dataset, the correlation between the 6 core genes and mitochondrial respiratory chain genes (|statistical|>4) was calculated. The results showed that MRPL12, PDK4, ACACB and GATM had the strongest correlation with mitochondrial respiration, and these 4 genes were selected as hub genes (Fig. 7C). The 6 mitochondrial respiratory chain genes most closely related to these 4 hub genes were then selected and a linear regression scatter plot was created. The results showed that MRPL12 was significantly positively correlated with TMEM186, UQCC3, COX7A1 and ATPAF1 (Fig. S3A), while PDK4, ACACB and GATM were positively correlated with COX7A1 and negatively correlated with TMEMI186, SDHAF3, UQCC3, COA7 and ATPAF1 (Fig. S3B-D). These results suggest that the core differential genes related to mitochondrial respiration are closely related to immune infiltrating cells in PCa.

Potential association of hub genes with DAMPs and mitochondrial metabolism. The TCGA-PRAD dataset was then used to create violin plots to determine the differences between DAMP-related genes (11 genes) and immune receptor-related genes (21 genes) in PCa and adjacent tissues. Genes with significant differences were selected for further research (P<0.001; Fig. 8A). An analysis of the correlation between the 4 hub genes and significantly different DAMP-related genes and immune receptors showed that they have a strong correlation (Fig. 8B). To further investigate the potential correlation between the 4 hub genes (MRPL12, PDK4, ACACB and GATM) and DAMPs and mitochondrial metabolism, the Mantel test was used to analyze statistical significance. The results showed that they were closely related to the mitochondrial metabolic

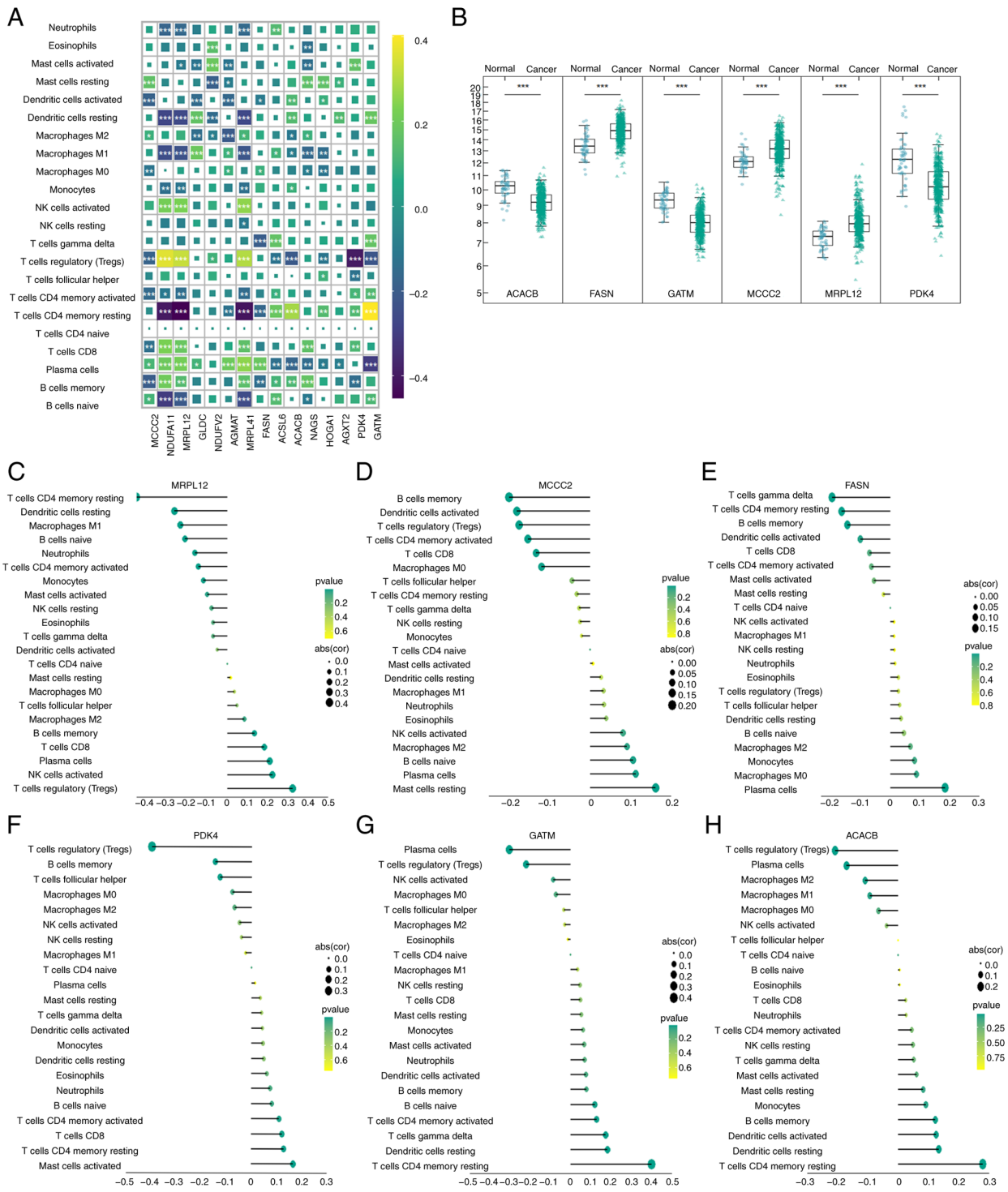

Figure 4. Relationship between core differential mitochondrial mRNA and tumor immune infiltration in PCa and normal prostate tissue. (A) TCGA-PRAD dataset was used to calculate the immune score of the transcripts per million expression matrix of PCa tissue (502 cases), which is shown as a heatmap. The genes on the x-axis are the core genes selected from TCGA-PRAD. The color of the heatmap represents the correlation coefficient. The larger the box is, the more statistically significant the correlation. (B) The box plot shows the 6 genes most closely related to immunity, with P-values determined by paired t-test. The R package ggplot2 was used to examine the correlation between hub genes and immune cells, with the results presented as lollipop plots. The relationship between (C) MRPL12, (D) MCCC2, (E) FASN, (F) PDK4, (G) GTAM and (H) ACACB with immune cell infiltration. The size of the points represents the absolute value of the correlation coefficient and the larger the points, the more correlated they are. The greener the point, the smaller the P-value. *P<0.05, **P<0.01, ***P<0.001. PCa, prostate cancer; TCGA, The Cancer Genome Atlas; PRAD, prostate adenocarcinoma; ACACB, acetyl-CoA carboxylase β; PDK4, pyruvate dehydrogenase kinase 4; GATM, glycine amidinotransferase; MCCC2, methylcrotonyl-CoA carboxylase subunit 2; MRPL12, mitochondrial ribosomal protein L12; FASN, fatty acid synthase.

pathways in gluconeogenesis, the tricarboxylic acid (TCA) cycle and pyruvate/ketone/lipid/amino acid metabolism in PCa (Fig. 8C).

Validating expression levels of DeMRGs. Finally, expression of the core genes was validated using the RWPE-1 (the non-PCa cell line used for comparison), PC-3, LNcap and

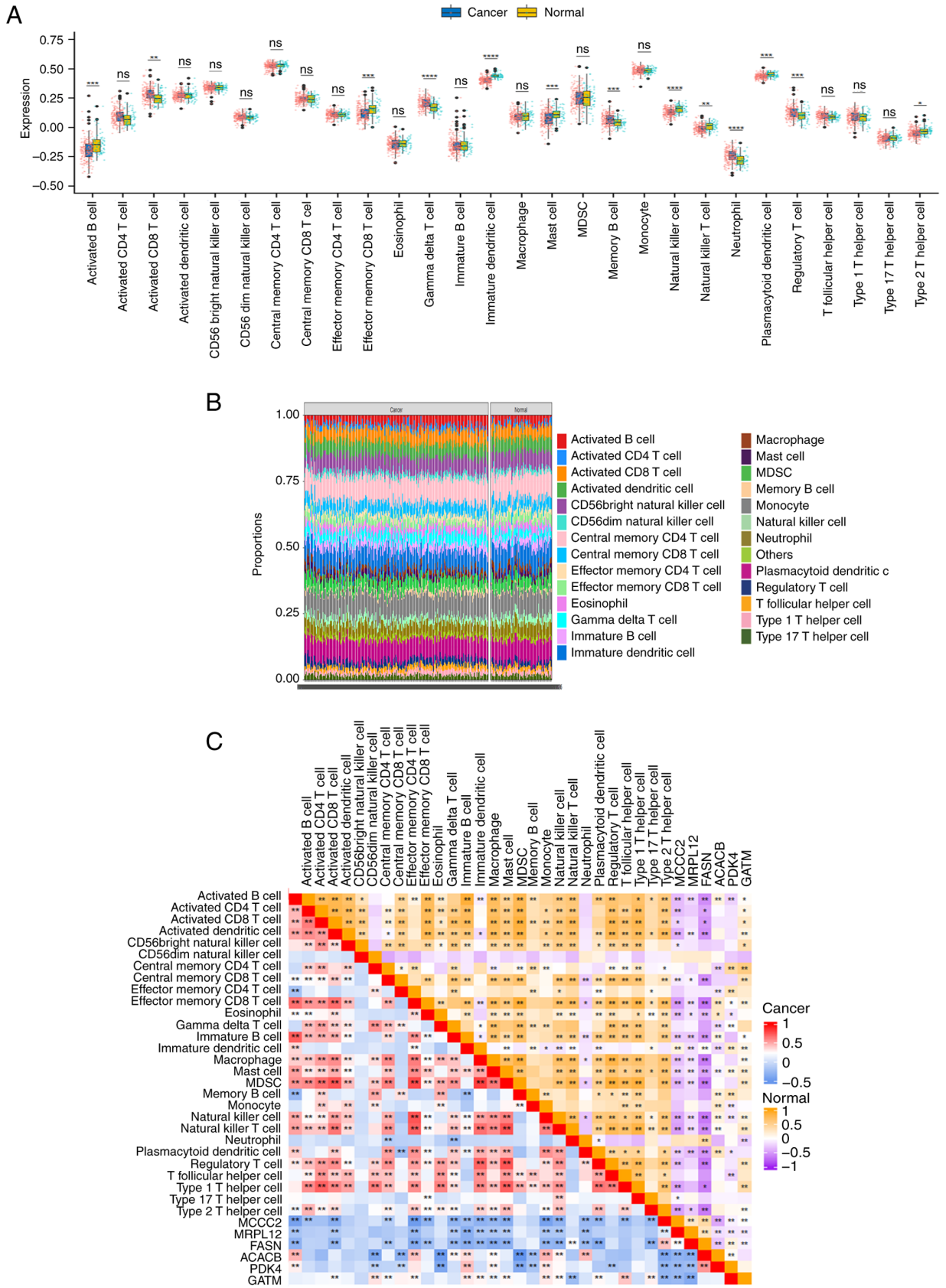

Figure 5. Validation of the relationship between MCCC2, MRPL12, FASN, PDK4, ACACB and GATM genes and tumor immunity in prostate cancer and normal prostate tissue. (A) Validation of the relationship between the MCCC2, MRPL12, FASN, PDK4, ACACB and GATM genes and tumor immunity in PCa and normal prostate tissue. The data is sourced from the validation dataset GSE70770. (B) The proportion of 26 immune cells in PCa and adjacent tissues in the validation dataset GSE70770. (C) The correlation between 6 core genes and immune cells in the validation dataset GSE70770. The darker the color, the stronger the correlation. The upper right corner shows the correlation between these genes and immune cells, while the lower left corner shows the correlation between these genes and immune cells in PCa. *P<0.05, **P<0.01, ***P<0.001; ****P<0.0001. ACACB, acetyl-CoA carboxylase β; PDK4, pyruvate dehydrogenase kinase 4; GATM, glycine amidinotransferase; MCCC2, methylcrotonyl-CoA carboxylase subunit 2; MRPL12, mitochondrial ribosomal protein L12; FASN, fatty acid synthase; PCa, prostate cancer.

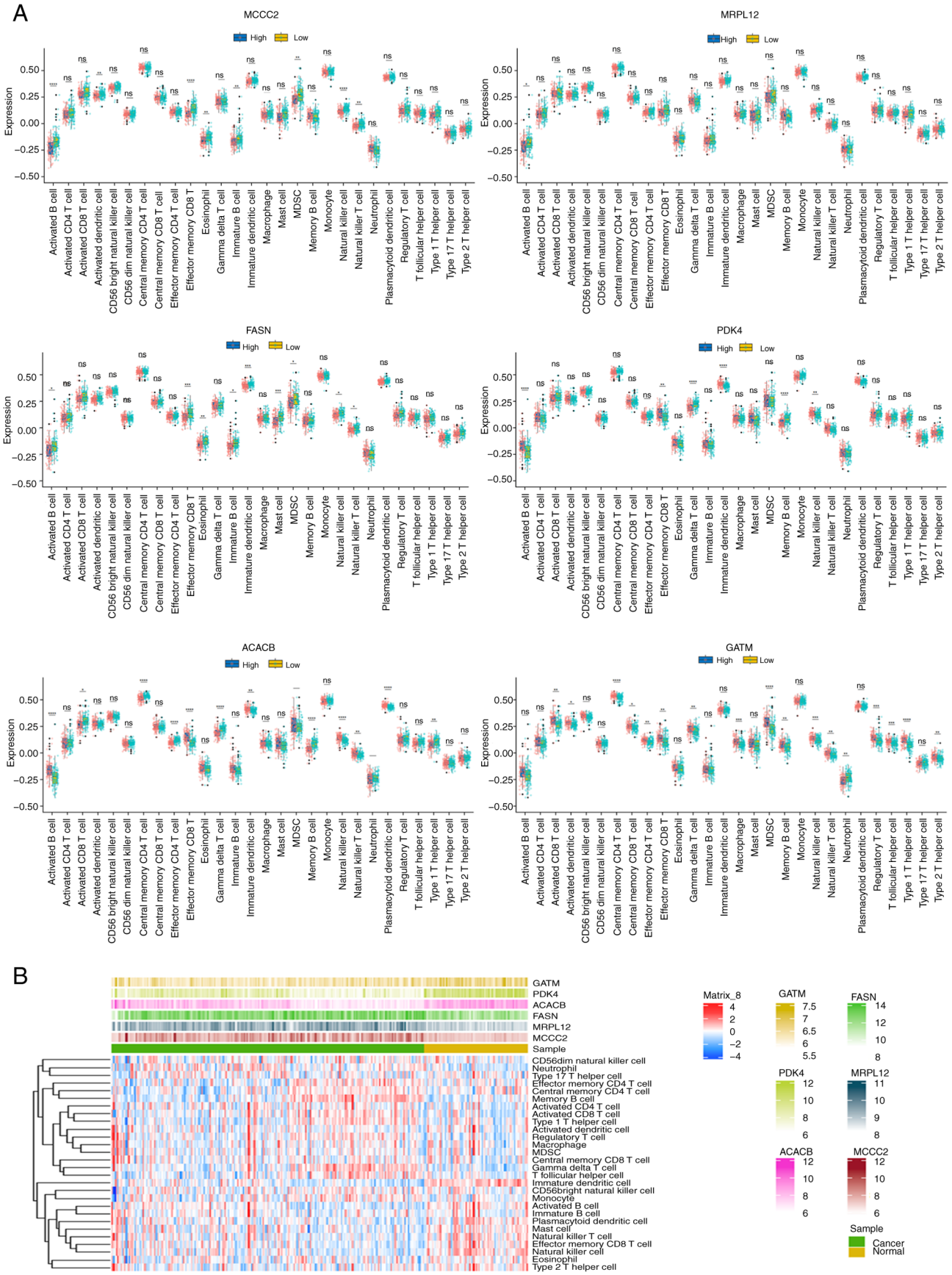

Figure 6. Validation of the relationship between the MCCC2, MRPL12, FASN, PDK4, ACACB and GATMM genes and immune cells in prostate cancer and normal prostate tissue. (A) The relationship between the core MCCC2, MRPL12, FASN, PDK4, ACACB and GATMM genes and immune cells, using the validation dataset GSE70770. (B) The differences between cancer and adjacent immune cells, as well as the relationship between the expression levels of the 6 core genes and immune cells, using the validation dataset GSE70770. *P<0.05, **P<0.01, ***P<0.001; ****P<0.0001. ns, no significance; ACACB, acetyl-CoA carboxylase β; PDK4, pyruvate dehydrogenase kinase 4; GATM, glycine amidinotransferase; MCCC2, methylcrotonyl-CoA carboxylase subunit 2; MRPL12, mitochondrial ribosomal protein L12; FASN, fatty acid synthase.

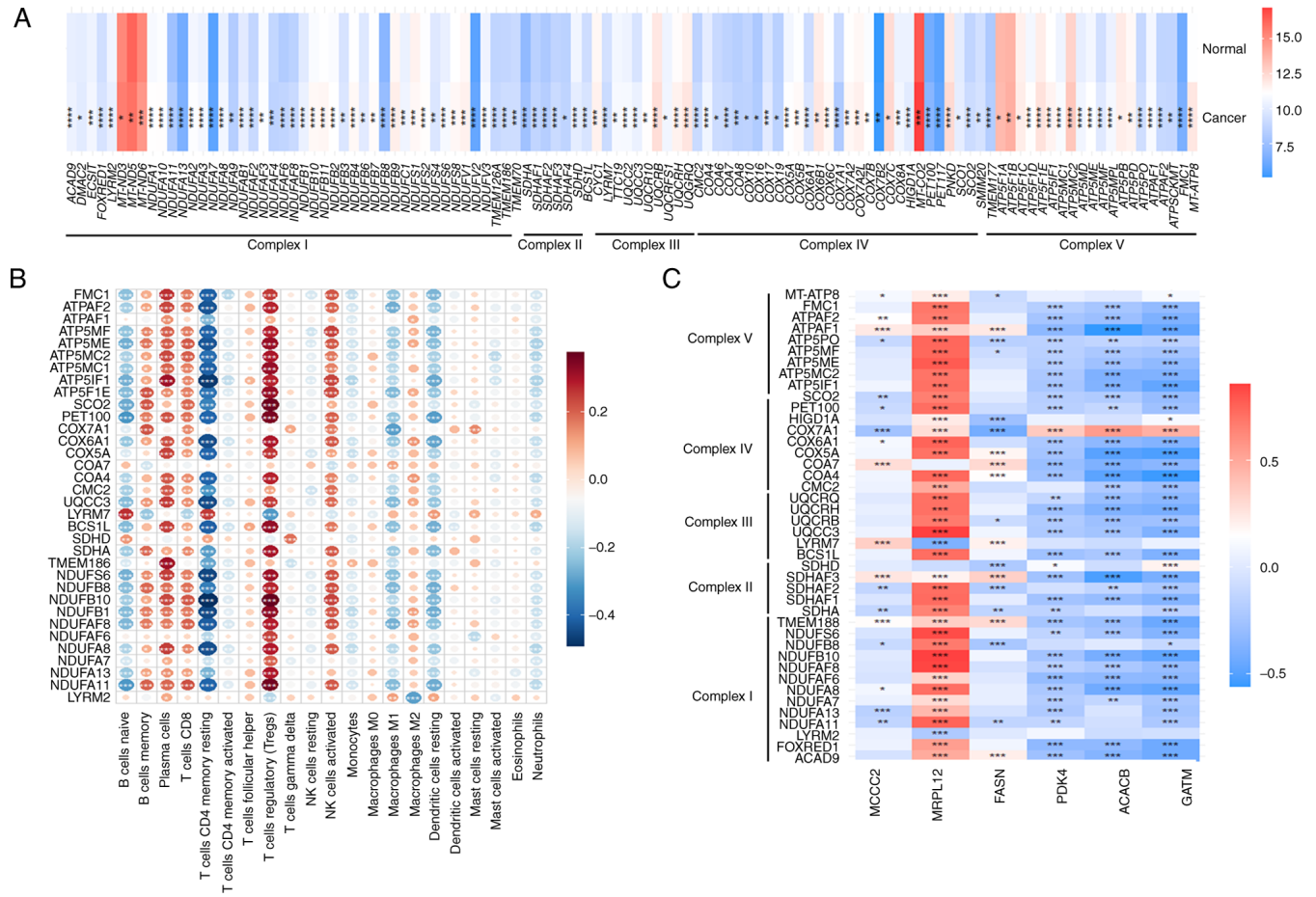

Figure 7. Relationship between mitochondrial respiration and prostate cancer. (A) Relationship between mitochondrial respiration and prostate cancer, as well as the relationship with 6 core genes. The dataset used is TCGA-PRAD. The genes of the five stages of mitochondrial respiration were provided by the MitoCarta 3.0 database, and statistically significant genes were screened out; (B) Using the TCGA-PRAD dataset, genes with |statistical|>6 from (A) were selected and the correlation between these genes and CIBERSORT immune infiltrating cells was calculated. (C) Using the TCGA-PRAD dataset, the correlation between the 6 core genes and mitochondrial respiratory chain genes (|statistical|>4) was calculated. *P<0.05, **P<0.01, ***P<0.001; ****P<0.0001. TCGA, The Cancer Genome Atlas; PRAD, prostate adenocarcinoma; ACACB, acetyl-CoA carboxylase β; PDK4, pyruvate dehydrogenase kinase 4; GATM, glycine amidinotransferase; MCCC2, methylcrotonyl-CoA carboxylase subunit 2; MRPL12, mitochondrial ribosomal protein L12; FASN, fatty acid synthase;

Du145 cell lines. The results showed that ACACB, PDK4 and GATM were downregulated in PCa, while MCCC2, MRPL12 and FASN were upregulated in PCa, consistent with the bioinformatics analysis (Fig. 9).

Discussion

Mitochondria are the 'power factories' in cells, providing 80% of the energy required for cellular life activities. Mitochondria play an important role in maintaining normal physiological metabolism and body development and are involved in the occurrence and development of various diseases (such as breast cancer and renal cell carcinoma) (19). Variations in mitochondrial DNA (mtDNA) sequences are common in certain tumors (such as ovarian cancer, oncocytoma and prostate cancer). Two types of mtDNA cancer variants can be identified: Novel mutations as oncogenic inducers and functional variants as adaptors, allowing cancer cells to grow in different environments. These mtDNA variants come from three sources: Familial variants, somatic mutations produced within each cell or individual and variants associated with ancient mtDNA lineages (haplotypes) that are considered to adapt to constantly changing tissues or geographical environments (20,21). In addition to mtDNA sequence mutations, mtDNA copy number and mtDNA sequence transfer to the nucleus may also lead to certain cancer types [such as breast epithelial cell lines, patient-derived xenograft models of triple-negative breast cancer and high-grade serous ovarian cancer (HGSC) and primary HGSC tumors] (22). There is a strong functional correlation between mtDNA mutations in eosinophilic tumors and PCa (21). In PCa, significant changes occur in the mitochondrial membrane, leading to the increased uptake of integrated membrane proteins. This process leads to increased rigidity and higher enzyme activity of cancer cell mitochondria (23). NKX3.1 is expressed in the prostate epithelium and its function is to protect the prostate from damage and inflammation as well as maintain the luminal prostate stem cells. In addition, it can regulate the expression of mitochondrial genes to promote mitochondrial homeostasis and prevent the occurrence of PCa (24).

Mitochondrial changes have a significant impact on the phenotype of prostate tumor cells. First, the progression of PCa is accompanied by an increase in ROS, which promotes its invasiveness. During the transformation and later stages

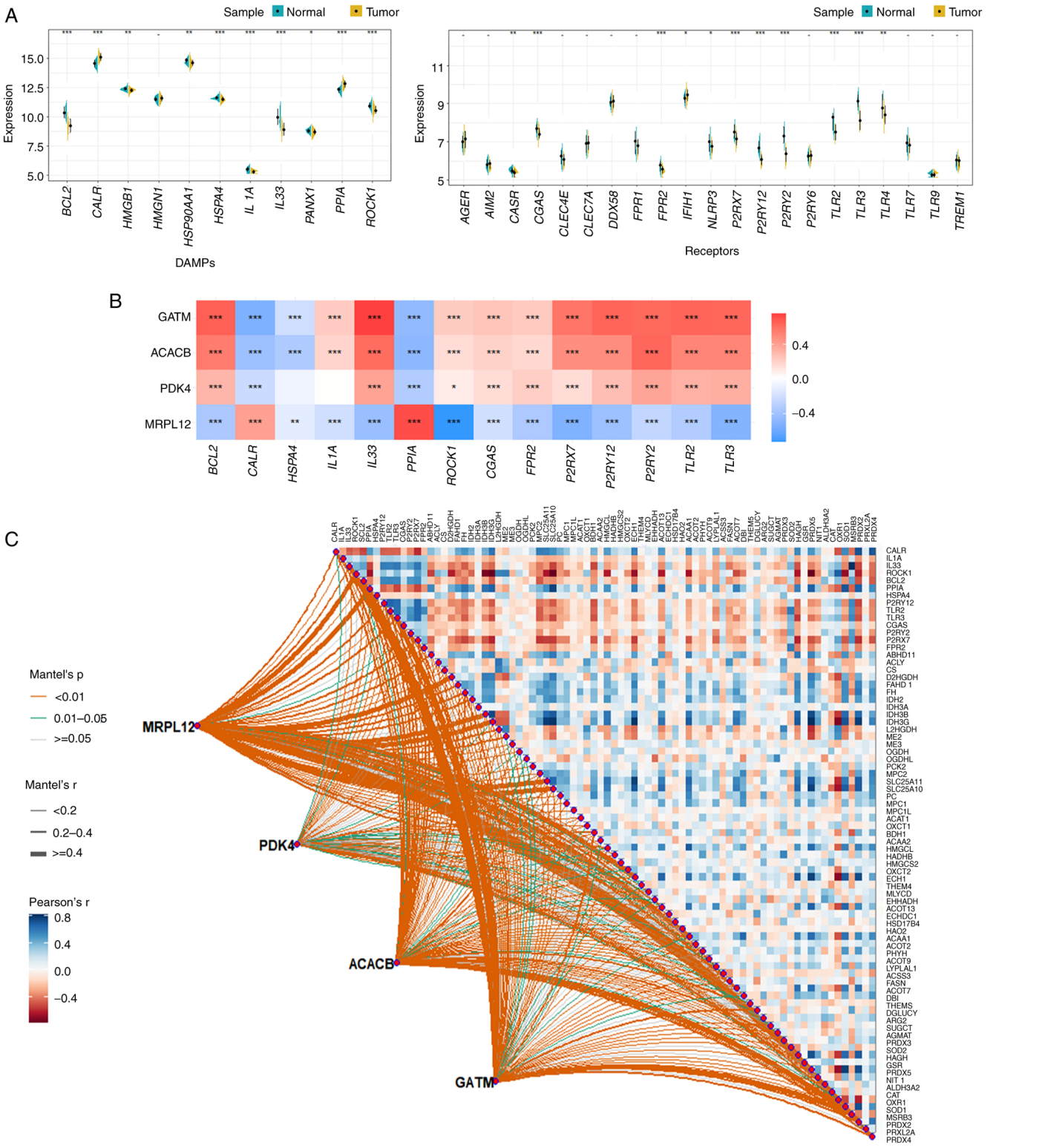

Figure 8. Potential correlation between 4 hub genes (MRPL12, PDK4, ACACB and GATM) and immune receptors and mitochondrial metabolism. (A) Using the TCGA-PRAD dataset, the differences between DAMP-related genes (11) and immune receptor-related genes (21) in PCa and adjacent tissues were detected; the genes with significant differences (**P<0.001) were selected for further study. (B) The correlation between the 4 hub genes and the significant differences in DAMP-related genes and immune receptors selected in (a). (C) Further investigation of the potential correlation between the 4 hub genes and DAMPs. *P<0.05, **P<0.01, ***P<0.001. PRAD, prostate adenocarcinoma; ACACB, acetyl-CoA carboxylase β; PDK4, pyruvate dehydrogenase kinase 4; GATM, glycine amidinotransferase; MCCC2, methylcrotonyl-CoA carboxylase subunit 2; MRPL12, mitochondrial ribosomal protein L12; FASN, fatty acid synthase; TCGA, The Cancer Genome Atlas.

of PCa development, PCa cells increase their mitochondrial respiration and glycolytic rates to meet energy needs. Due to enhanced mitochondrial respiration, ROS levels increase, inducing signaling pathways related to PCa growth and survival (25-27). Mitochondrial respiration and metabolism are related to PCa, while normal prostate epithelial cells

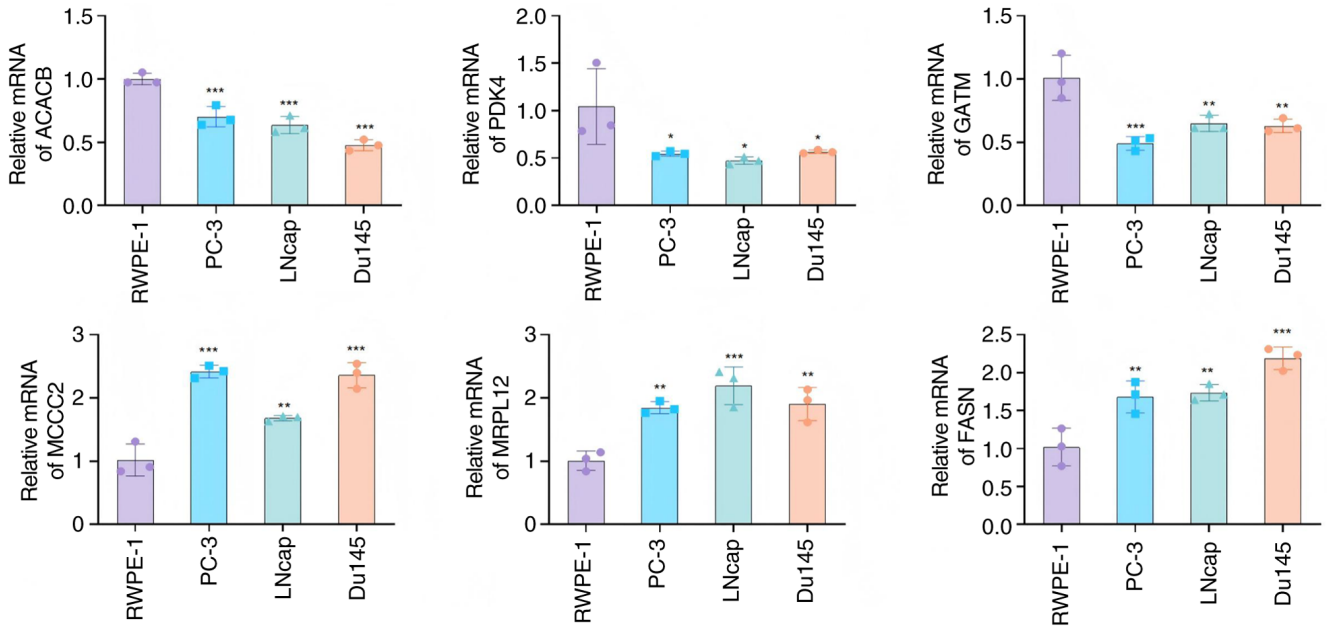

Figure 9. RT-qPCR validation of the core genes. Relative RNA levels of ACACB, PDK4, GATM, MCCC2, MRPL12 and FASN were determined by the RT-qPCR for the RWPE-1, PC-3, LNcap and Du145 cell lines. *P<0.05, **P<0.01, ***P<0.001; n=3. RT-qPCR, reverse transcription-quantitative PCR; ACACB, acetyl-CoA carboxylase β; PDK4, pyruvate dehydrogenase kinase 4; GATM, glycine amidinotransferase; MCCC2, methylcrotonyl-CoA carboxylase subunit 2; MRPL12, mitochondrial ribosomal protein L12; FASN, fatty acid synthase.

are highly dependent on glycolysis and produce citrate from glucose. TCA cycle cannot effectively produce a large amount of citrate. During the transformation process, PCa cells gradually reactivate OXPHOS, increase glucose metabolism and reduce citrate production. In addition, the late stages of PCa are marked by an increase in TCA cycle and citrate levels, which are used by cancer cells for biomolecular synthesis to support their growth (28). Epithelial-mesenchymal transition (EMT) provides enhanced migration and invasion capabilities for cancer cells, promoting tumor dissemination and metastasis. A study has shown that the downregulation of mitochondrial proteins involved in OXPHOS is associated with increased EMT and invasive disease characteristics (29). The changes in mitochondrial gene expression are also related to the growth, survival and drug resistance of PCa. Previous research has found that mitochondrial fission factor and dynamic related protein-1 are amplified in castration-resistant PCa, leading to low patient survival rates (29). In addition to serving as a power source for cells, mitochondria also play an important role in cell death pathways, such as apoptosis. Mitochondria are crucial in the activation of cell apoptosis through intrinsic pathways in response to excessive oxidative stress and DNA damage (30,31). Higher expression of Bcl-x is associated with higher-grade PCa tumors, as well as the presence of lymph node metastasis and distant metastasis. Given that Bcl-x is a key regulator of mitochondrial-mediated apoptosis, these findings further indicate that mitochondria play an important role in PCa immune escape (32,33).

In PCa, ARs reprogram the entire cellular metabolic pathway, including aerobic glycolysis and mitochondrial respiration, as well as *de novo* fat generation, to support the metabolic and biosynthetic needs of PCa cells (34,35). The m6A-mediated circular RNA (circ)RBM33-FMR1 complex can activate mitochondrial metabolism by stabilizing pyruvate dehydrogenase E1 subunit α1 mRNA, thereby promoting the progression of PCa and reducing the arylsulfatase family member I efficacy of circRBM33 in PCa treatment (36). Treatment targeting mitochondria may help with PCa as the naturally occurring amino acid 5-aminolevulinic acid (5-ALA) immediately enhances mitochondrial ROS production after exposure to IR and reduces mitochondrial membrane potential by increasing intracellular PpIX (the metabolite of 5-ALA) in PC-3 and DU-145 PCA cell lines. IR is accompanied by mitochondrial dysfunction induced by 5-ALA and an increase in ATP production, which switches energy metabolism to a quiescent state. Under hypoxic conditions, IR induces ROS burst and mitochondrial dysfunction with 5-ALA to reduce cancer stemness and radiation resistance (37). RNA polymerase mitochondria (POLRMT) are crucial for mitochondrial transcription mechanisms and other mitochondrial functions. Upregulated POLRMT is important for PCa cell growth and mitochondrial POLRMT may serve as a target for PCa treatment (38).

In the present study, MRPL12, PDK4, ACACB and GATM were identified as hub genes. MRPL12 is a core component of the mitochondrial ribosome (mitoribosome), which is essential for synthesizing proteins encoded by mtDNA, including key subunits of the OXPHOS complex (39). In hepatocellular carcinoma, MRPL12 is upregulated via the PI3K/mTOR/YY1 pathway, which enhances OXPHOS and mitochondrial DNA content, thereby driving malignant phenotypes (39). PDK4 is a gene involved in fatty acid metabolism. Together with ACACB, FABP3 and other genes, it constitutes a metabolic gene signature for prostate cancer. By inhibiting the activity of the pyruvate dehydrogenase complex, PDK4 promotes glycolysis and suppresses OXPHOS, thereby supporting the

Warburg effect in tumors (40). Following androgen receptor inhibition, PCa cells switch to a dependence on mitochondrial oxidative metabolism, and PDK4 may play a regulatory role in this process (41). ACACB is a rate-limiting enzyme in fatty acid synthesis and is involved in lipid metabolic reprogramming in prostate cancer. As a member of the same 5-gene metabolic signature as PDK4, its low expression is associated with high-risk PCa (40). Dysregulated lipid metabolism may promote immune evasion by altering the function of immune cells (such as $CD8^+$ T cells) in the tumor microenvironment (42). GATM is involved in creatine synthesis, and its expression is associated with the MYC pathway and OXPHOS. In PCa, high GATM expression may lead to mitochondrial dysfunction (such as reduced aspartate levels), driving metabolic shifts toward glycolysis (43).

Despite the novel findings regarding mitochondrial hub genes in PCa, the present study has several limitations that should be acknowledged. First, the identification and validation of DeMRGs and hub genes relied heavily on publicly available datasets (TCGA-PRAD, GSE46602, GSE55945 and GSE70770) and *in vitro* experiments using established PCa cell lines (Du145, PC-3 and LNcap) and a normal prostate epithelial cell line (RWPE-1). The lack of primary PCa tissue samples from a patient cohort (such as clinical specimens with detailed pathological staging, treatment history and long-term follow-up data) limits the generalizability of the results to diverse clinical populations, as public datasets may have inherent biases in sample selection and data standardization. Second, the functional validation of the four hub genes (MRPL12, PDK4, ACACB and GATM) was limited to correlative analyses (such as associations with immune cell infiltration, mitochondrial respiration and metabolic pathways) and gene expression verification via RT-qPCR. No in-depth mechanistic experiments were performed to elucidate the direct roles of these hub genes in PCa progression, for instance, gain-of-function/loss-of-function assays (such as overexpression plasmids, small interfering RNA or CRISPR-Cas9) to assess changes in PCa cell proliferation, migration, invasion or mitochondrial function (such as mitochondrial membrane potential, ROS production and ATP levels) were not conducted. Additionally, *in vivo* validation using PCa xenograft models or genetically engineered mouse models was absent, which would be critical to confirm the *in vivo* relevance of these hub genes. In summary, while the present study provides a foundation for understanding the role of mitochondrial hub genes in PCa, future studies addressing these limitations, including large-scale clinical validation, mechanistic experiments and subtype-specific analyses, will be necessary to advance the translational potential of the findings.

In summary, the present study found that ACACB, PDK4 and GATM were downregulated, while MCCC2, MRPL12 and FASN are upregulated in PCa; among these genes, MCCC2 and FASN were linked to adverse PCa phenotypes and MRPL12, PDK4, ACACB and GATM showed the strongest associations with mitochondrial metabolic pathways in PCa, providing potential therapeutic targets for PCa treatment.

Acknowledgements

Not applicable.

Funding

This work was supported by Hunan Provincial Natural Science Foundation of China (grant nos. 2025JJ50553 and 2025JJ80574) and Changsha Municipal Natural Science Foundation (grant no. kq2502330).

Availability of data and materials

The data generated in the present study may be requested from the corresponding author.

Authors' contributions

SL and HS conducted most experiments and wrote the manuscript. LH, LL, YW conceived, designed and interpreted data. All authors edited the manuscript. All authors read and approved the final version of the manuscript. SL and HS confirm the authenticity of all the raw data

Ethics approval and consent to participate

Not applicable.

Patient consent for publication

Not applicable.

Competing interests

The authors declare that they have no competing interests.

References

1. Bray F, Laversanne M, Sung H, Ferlay J, Siegel RL, Soerjomataram I and Jemal A: Global cancer statistics 2022: GLOBOCAN estimates of incidence and mortality worldwide for 36 cancers in 185 countries. CA Cancer J Clin 74: 229-263, 2024.
2. Moris L, Cumberbatch MG, Van den Broeck T, Gandaglia G, Fossati N, Kelly B, Pal R, Briers E, Cornford P, De Santis M, *et al*: Benefits and risks of primary treatments for High-risk localized and locally advanced prostate cancer: An international multidisciplinary systematic review. Eur Urol 77: 614-627, 2020.
3. Rebello RJ, Oing C, Knudsen KE, Loeb S, Johnson DC, Reiter RE, Gillessen S, Van der Kwast T and Bristow RG: Prostate cancer. Nat Rev Dis Primers 7: 9, 2021.
4. Schaeffer E, Srinivas S, Antonarakis ES, Armstrong AJ, Bekelman JE, Cheng H, D'Amico AV, Davis BJ, Desai N, Dorff T, *et al*: NCCN guidelines insights: Prostate cancer, version 1.2021. J Natl Compr Canc Netw 19: 134-143, 2021.
5. Linder S, van der Poel HG, Bergman AM, Zwart W and Prekovic S: Enzalutamide therapy for advanced prostate cancer: Efficacy, resistance and beyond. Endocr Relat Cancer 26: R31-R52, 2018.
6. Parida S, Pal I, Parekh A, Thakur B, Bharti R, Das S and Mandal M: GW627368X inhibits proliferation and induces apoptosis in cervical cancer by interfering with EP4/EGFR interactive signaling. Cell Death Dis 7: e2154, 2016.
7. Sathya S, Sudhagar S, Sarathkumar B and Lakshmi BS: EGFR inhibition by pentacyclic triterpenes exhibit cell cycle and growth arrest in breast cancer cells. Life Sci 95: 53-62, 2014.
8. Kang H, Kim B, Park J, Youn H and Youn B: The Warburg effect on radioresistance: Survival beyond growth. Biochim Biophys Acta Rev Cancer 1878: 188988, 2023.
9. Chen H, Zhou L, Wu X, Li R, Wen J, Sha J and Wen X: The PI3K/AKT pathway in the pathogenesis of prostate cancer. Front Biosci (Landmark Ed) 21: 1084-1091, 2016.

10. Kumar R, Srinivasan S, Pahari P, Rohr J and Damodaran C: Activating stress-activated protein kinase-mediated cell death and inhibiting epidermal growth factor receptor signaling: A promising therapeutic strategy for prostate cancer. Mol Cancer Ther 9: 2488-2496, 2010.
11. Wu W, Yang Q, Fung KM, Humphreys MR, Brame LS, Cao A, Fang YT, Shih PT, Kropp BP and Lin HK: Linking γ-aminobutyric acid A receptor to epidermal growth factor receptor pathways activation in human prostate cancer. Mol Cell Endocrinol 383: 69-79, 2014.
12. Hirokawa N, Noda Y, Tanaka Y and Niwa S: Kinesin superfamily motor proteins and intracellular transport. Nat Rev Mol Cell Biol 10: 682-696, 2009.
13. Drechsler H and McAinsh AD: Kinesin-12 motors cooperate to suppress microtubule catastrophes and drive the formation of parallel microtubule bundles. Proc Natl Acad Sci USA 113: E1635-E1644, 2016.
14. Zhao H, Bo Q, Wu Z, Liu Q, Li Y, Zhang N, Guo H and Shi B: KIF15 promotes bladder cancer proliferation via the MEK-ERK signaling pathway. Cancer Manag Res 11: 1857-1868, 2019.
15. Livak KJ and Schmittgen TD: Analysis of relative gene expression data using real-time quantitative PCR and the 2(-Delta Delta C(T)) method. Methods 25: 402-408, 2001.
16. Mortensen MM, Høyer S, Lynnerup AS, Ørntoft TF, Sørensen KD, Borre M and Dyrskjøt L: Expression profiling of prostate cancer tissue delineates genes associated with recurrence after prostatectomy. Sci Rep 5: 16018, 2015.
17. Arredouani MS, Lu B, Bhasin M, Eljanne M, Yue W, Mosquera JM, Bubley GJ, Li V, Rubin MA, Libermann TA and Sanda MG: Identification of the transcription factor single-minded homologue 2 as a potential biomarker and immunotherapy target in prostate cancer. Clin Cancer Res 15: 5794-5802, 2009.
18. Ross-Adams H, Lamb AD, Dunning MJ, Halim S, Lindberg J, Massie CM, Egevad LA, Russell R, Ramos-Montoya A, Vowler SL, *et al*: Integration of copy number and transcriptomics provides risk stratification in prostate cancer: A discovery and validation cohort study. EBioMedicine 2: 1133-1144, 2015.
19. Hocaoglu H and Sieber M: Mitochondrial respiratory quiescence: A new model for examining the role of mitochondrial metabolism in development. Semin Cell Dev Biol 138: 94-103, 2023.
20. Boso D, Piga I, Trento C, Minuzzo S, Angi E, Iommarini L, Lazzarini E, Caporali L, Fiorini C, D'Angelo L, *et al*: Pathogenic mitochondrial DNA variants are associated with response to anti-VEGF therapy in ovarian cancer PDX models. J Exp Clin Cancer Res 43: 325, 2024.
21. Kopinski PK, Singh LN, Zhang S, Lott MT and Wallace DC: Mitochondrial DNA variation and cancer. Nat Rev Cancer 21: 431-445, 2021.
22. Kim M, Gorelick AN, Vàzquez-García I, Williams MJ, Salehi S, Shi H, Weiner AC, Ceglia N, Funnell T, Park T, *et al*: Single-cell mtDNA dynamics in tumors is driven by coregulation of nuclear and mitochondrial genomes. Nat Genet 56: 889-899, 2024.
23. Zichri SB, Kolusheva S, Shames AI, Schneiderman EA, Poggio JL, Stein DE, Doubijensky E, Levy D, Orynbayeva Z and Jelinek R: Mitochondria membrane transformations in colon and prostate cancer and their biological implications. Biochim Biophys Acta Biomembr 1863: 183471, 2021.
24. Papachristodoulou A, Rodriguez-Calero A, Panja S, Margolskee E, Virk RK, Milner TA, Martina LP, Kim JY, Di Bernardo M, Williams AB, *et al*: NKX3.1 Localization to mitochondria suppresses prostate cancer initiation. Cancer Discov 11: 2316-2333, 2021.
25. Mamouni K, Kallifatidis G and Lokeshwar BL: Targeting mitochondrial metabolism in prostate cancer with triterpenoids. Int J Mol Sci 22: 2466, 2021.
26. Chen CL, Lin CY and Kung HJ: Targeting mitochondrial OXPHOS and their regulatory signals in prostate cancers. Int J Mol Sci 22: 13435, 2021.
27. Han C, Wang Z, Xu Y, Chen S, Han Y, Li L, Wang M and Jin X: Roles of reactive oxygen species in biological behaviors of prostate cancer. Biomed Res Int 2020: 1269624, 2020.
28. Wang H, Li N, Liu Q, Guo J, Pan Q, Cheng B, Xu J, Dong B, Yang G, Yang B, *et al*: Antiandrogen treatment induces stromal cell reprogramming to promote castration resistance in prostate cancer. Cancer Cell 41: 1345-1362.e9, 2023.
29. Guerra F, Guaragnella N, Arbini AA, Bucci C, Giannattasio S and Moro L: Mitochondrial dysfunction: A novel potential driver of Epithelial-to-mesenchymal transition in cancer. Front Oncol 7: 295, 2017.
30. Civenni G, Bosotti R, Timpanaro A, Vàzquez R, Merulla J, Pandit S, Rossi S, Albino D, Allegrini S, Mitra A, *et al*: Epigenetic control of mitochondrial fission enables Self-renewal of stem-like tumor cells in human prostate cancer. Cell Metab 30: 303-318.e6, 2019.
31. Jeong SY and Seol DW: The role of mitochondria in apoptosis. BMB Rep 41: 11-22, 2008.
32. Castilla C, Congregado B, Chinchón D, Torrubia FJ, Japón MA and Sáez C: Bcl-xL is overexpressed in hormone-resistant prostate cancer and promotes survival of LNCaP cells via interaction with proapoptotic Bak. Endocrinology 147: 4960-4967, 2006.
33. Krajewska M, Krajewski S, Epstein JI, Shabaik A, Sauvageot J, Song K, Kitada S and Reed JC: Immunohistochemical analysis of bcl-2, bax, bcl-X, and mcl-1 expression in prostate cancers. Am J Pathol 148: 1567-1576, 1996.
34. Massie CE, Lynch A, Ramos-Montoya A, Boren J, Stark R, Fazli L, Warren A, Scott H, Madhu B, Sharma N, *et al*: The androgen receptor fuels prostate cancer by regulating central metabolism and biosynthesis. EMBO J 30: 2719-2733, 2011.
35. Audet-Walsh É, Dufour CR, Yee T, Zouanat FZ, Yan M, Kalloghlian G, Vernier M, Caron M, Bourque G, Scarlata E, *et al*: Nuclear mTOR acts as a transcriptional integrator of the androgen signaling pathway in prostate cancer. Genes Dev 31: 1228-1242, 2017.
36. Zhong C, Long Z, Yang T, Wang S, Zhong W, Hu F, Teoh JY, Lu J and Mao X: M6A-modified circRBM33 promotes prostate cancer progression via PDHA1-mediated mitochondrial respiration regulation and presents a potential target for ARSI therapy. Int J Biol Sci 19: 1543-1563, 2023.
37. Owari T, Tanaka N, Nakai Y, Miyake M, Anai S, Kishi S, Mori S, Fujiwara-Tani R, Hojo Y, Mori T, *et al*: 5-Aminolevulinic acid overcomes hypoxia-induced radiation resistance by enhancing mitochondrial reactive oxygen species production in prostate cancer cells. Br J Cancer 127: 350-363, 2022.
38. Li X, Yao L, Wang T, Gu X, Wu Y and Jiang T: Identification of the mitochondrial protein POLRMT as a potential therapeutic target of prostate cancer. Cell Death Dis 14: 665, 2023.
39. Ji X, Yang Z, Li C, Zhu S, Zhang Y, Xue F, Sun S, Fu T, Ding C, Liu Y, *et al*: Mitochondrial ribosomal protein L12 potentiates hepatocellular carcinoma by regulating mitochondrial biogenesis and metabolic reprogramming. Metabolism 152: 155761, 2023.
40. Fan Y, Wang J, Wang Y, Li Y, Wang S, Weng Y, Yang Q, Chen C, Lin L, Qiu Y, *et al*: Development and clinical validation of a novel 5 gene signature based on fatty acid Metabolism-related genes in oral squamous cell carcinoma. Oxid Med Cell Longev 2022: 3285393, 2022.
41. Crowell PD, Giafaglione JM, Jones AE, Nunley NM, Hashimoto T, Delcourt AML, Petcherski A, Agrawal R, Bernard MJ, Diaz JA, *et al*: MYC is a regulator of androgen receptor inhibition-induced metabolic requirements in prostate cancer. Cell Rep 42: 113221, 2023.
42. Li L, Chao Z, Peng H, Hu Z, Wang Z and Zeng X: Tumor ABCC4-mediated release of PGE2 induces CD8+ T cell dysfunction and impairs PD-1 blockade in prostate cancer. Int J Biol Sci 20: 4424-4437, 2024.
43. Löf C, Sultana N, Goel N, Heron S, Wahlström G, House A, Holopainen M, Käkelä R and Schleutker J: ANO7 expression in the prostate modulates mitochondrial function and lipid metabolism. Cell Commun Signal 23: 71, 2025.